[9]Bailey, A. B. and Sims, W. H., "The Shock Shape and Shock Detachment Distance for Spheres and Flat-Faced Bodies in Low Density, Hypervelocity Argon Flow," Arnold Engineering Development Center, Tenn., Rept. AEDC-TDR-63-21, 1963.

Application of Brittle Coatings to Graphite Fiber-Reinforced Plastics

R. Prabhakaran*
Indian Institute of Technology, Kanpur, India

Nomenclature

E = Young's modulus
G = shear modulus
K = ratio of compressive strength of brittle coating to its tensile strength
S = composite compliance
γ = shear strain
ϵ = normal strain
ν = Poisson's ratio
σ = normal stress
τ = shear stress
θ = angle between L and x directions
θ' = angle between L direction and calibration beam axis
ϕ = angle between major principal stress and major principal strain

Subscripts

$1,L$ = direction of major amount of reinforcement in the composite
$2,T$ = direction transverse to the L direction in the plane of the composite
t = threshold
x = direction of the major principal strain in the composite
y = direction of the minor principal strain in the composite

Superscripts

C = brittle coating
S = specimen or structure made of composite material
$*$ = at the time of failure of the brittle coating
$'$ = for the calibration beam axes

Introduction

THE brittle coating method of stress analysis has the advantage of being a whole field method. While the magnitudes of the stresses determined by this method are subject to considerable error due to the many variables influencing the coating behavior, the directions of the principal strains are obtained easily and accurately. The number of strain gages required for measurement of stress can be reduced by determination of the principal directions with a brittle coating. With the increasing use of structures fabricated from advanced composites such as graphite fiber-reinforced plastics, there is a need to update the conventional methods of experimental stress analysis. Photo-orthotropic-elasticity[1] is one such development.

Received March 8, 1978; revision received Aug. 7, 1978.

Index categories: Structural Composite Materials; Structural Statics.

*Assistant Professor, Dept. of Mechanical Engineering.

The stress transfer from a structure fabricated from a composite material to a brittle coating is examined here. The failure of the coating according to the Mohr theory of failure is studied and results are presented for the case of brittle coating applied to a unidirectionally reinforced graphite-epoxy composite structure.

Analysis

The most frequently employed relationship[2] for the interpretation of brittle coating data in the case of isotropic structures is the simple equation

$$\sigma_1^s = E^s \epsilon_1^* \tag{1}$$

This relationship totally neglects the biaxial effects due to σ_2^s. In calibration,

$$\sigma_2^s = 0, \quad \epsilon_2^s = -\nu^s \epsilon_1^s \tag{2}$$

However, in practice σ_2^s and ϵ_2^s may have any value with respect to σ_1^s and ϵ_1^s. The effect of some of the variables, such as the strength ratio K and the Poisson's ratio mismatch, on the failure of the coating is shown in Ref. 2.

When a brittle coating is applied to an anisotropic structure, the analysis proceeds on the same lines as in the case of the isotropic structure: the principal strain directions for the structure and for the coating are assumed to be the same, and the strains are assumed to be transmitted faithfully from the structure to the coating. The plane state of stress produced in the coating by the plane state of stress acting on the surface of the composite structure can be represented by

$$\sigma_x^c = \frac{E^c}{1-(\nu^c)^2}\left[\sigma_x^s (A + B\nu^c) + \sigma_y^s (B + D\nu^c)\right] \tag{3}$$

$$\sigma_y^c = \frac{E^c}{1-(\nu^c)^2}\left[\sigma_x^s (A\nu^c + B) + \sigma_y^s (B\nu^c + D)\right] \tag{4}$$

where

$$A = \overline{S_{11}} - \frac{\overline{S_{16}}}{\overline{S_{66}}}\overline{S_{16}}, \quad B = \overline{S_{12}} - \frac{\overline{S_{16}}}{\overline{S_{66}}}\overline{S_{26}}, \quad D = \overline{S_{22}} - \frac{\overline{S_{26}}}{\overline{S_{66}}}\overline{S_{26}} \tag{5}$$

and $\overline{S_{11}}$, $\overline{S_{12}}$,... etc., are the composite compliances transformed to the principal strain axes, making an angle θ with the material symmetry axes.

If the brittle coating calibration is performed in the usual manner on beams prepared from the same composite material as the structure, with the angle between the beam axis and the direction of major reinforcement varied from 0 to 90 deg, we can write

$$\sigma_{x'}^s = \epsilon_{x'}^s / \overline{S_{11}'}, \quad \sigma_{y'}^s = 0 \text{ and } \epsilon_{x'}^s = \epsilon_t^* \tag{6}$$

Substituting Eqs. (6) in Eqs. (3) and (4), the coating stresses in the calibration beam are given by

$$\sigma_x^c = \frac{E^c}{1-(\nu^c)^2}\left[(A + B\nu^c)\sigma_x^*\right] \tag{7}$$

$$\sigma_y^c = \frac{E^c}{1-(\nu^c)^2}\left[(A\nu^c + B)\sigma_x^*\right] \tag{8}$$

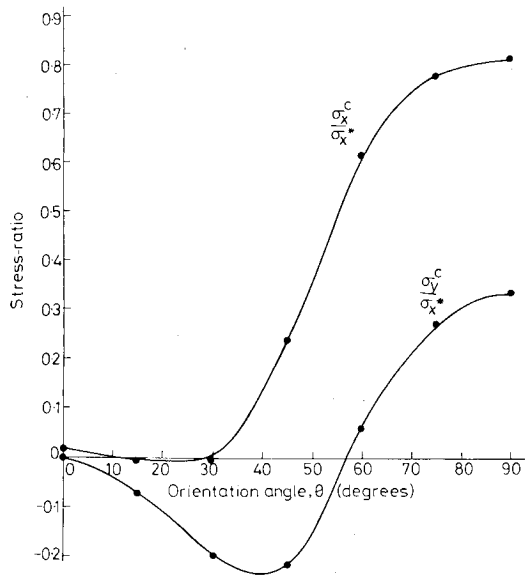

Fig. 1 Coating stresses in the composite calibration beams.

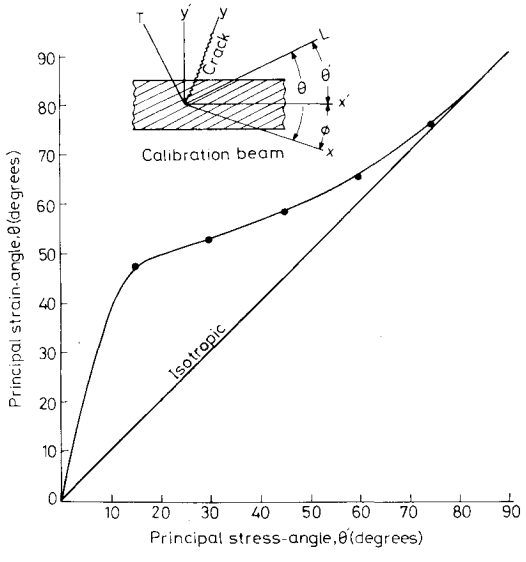

Fig. 2 Difference between principal stress and principal strain directions in unidirectional graphite-epoxy calibration beams.

The principal strains and principal stresses for the composite are not in the same direction, except when the beam axis coincides with one of the material symmetry axes. Therefore, the cracks in the brittle coating will be inclined at an angle $[(\pi/2)-\phi]$ with the beam axis, instead of $\pi/2$, where

$$\tan 2\phi = -\overline{S_{16}}' / (\overline{S_{11}}' - \overline{S_{12}}') \tag{9}$$

The failure of the coating in a biaxial stress-field can be investigated by employing the Mohr theory of failure. For the case of biaxial tension ($\sigma_x^c \geq \sigma_y^c \geq 0$), the failure equation can be obtained as

$$\frac{\sigma_x^s}{\sigma_x^*} + \frac{\sigma_y^s}{\sigma_x^*}\left(\frac{B+D\nu^c}{A+B\nu^c}\right) \geq 1 \tag{10}$$

For the case of tension-compression ($\sigma_x^c \geq 0 \geq \sigma_y^c$),

$$\frac{\sigma_x^s}{\sigma_x^*}\left[1 - \frac{A\nu^c+B}{K(A+B\nu^c)}\right] + \frac{\sigma_y^s}{\sigma_x^*}\left[\frac{B+D\nu^c}{A+B\nu^c} - \frac{B\nu^c+D}{K(A+B\nu^c)}\right] \geq 1 \tag{11}$$

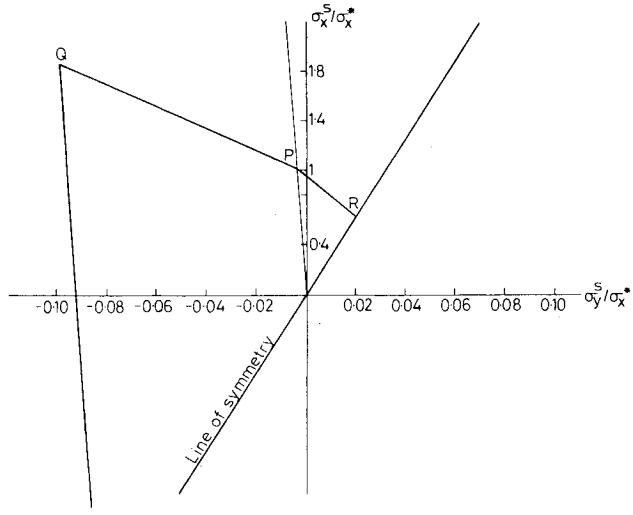

Fig. 3 Failure curves for $\theta = 0$ deg.

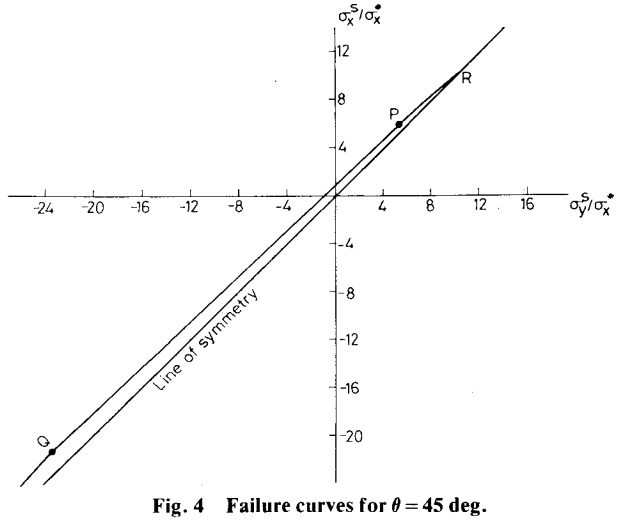

Fig. 4 Failure curves for $\theta = 45$ deg.

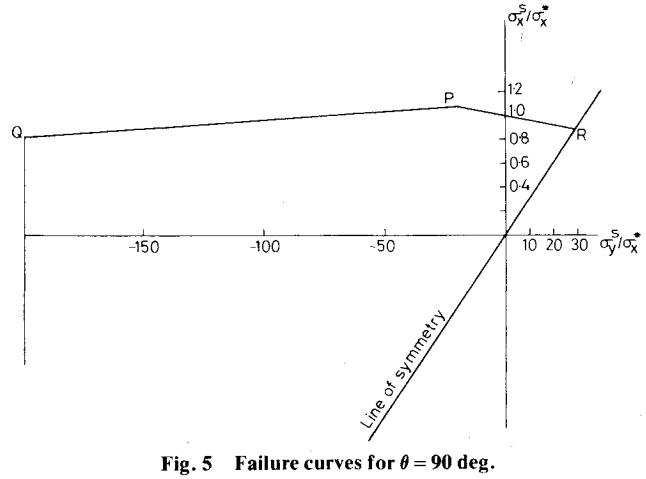

Fig. 5 Failure curves for $\theta = 90$ deg.

The failure condition for the case of biaxial compression ($0 \geq \sigma^c{}_x \geq \sigma_y^c$) is given by

$$-\left[\frac{\sigma_x^s}{\sigma_x^*}\left(\frac{A\nu^c+B}{A+B\nu^c}\right) + \frac{\sigma_y^s}{\sigma_x^*}\left(\frac{B\nu^c+D}{A+B\nu^c}\right)\right] \geq K \tag{12}$$

Results and Conclusions

Results have been obtained for unidirectionally reinforced graphite-epoxy material, with the following elastic proper-

ties[3]: $E_L = 30 \times 10^6$ psi $= 20.80 \times 10^4$ MPa, $E_T = 0.75 \times 10^6$ psi $= 0.52 \times 10^4$ MPa, $G_{LT} = 0.375 \times 10^6$ psi'0.26×10^4 MPa, and $\nu_{LT} = 0.25$. The variation of the coating stresses with the orientation of the calibration beam is shown in Fig. 1. The coating stresses are in general relatively high in comparison to the calibration beam stresses for angles greater than 45 deg. It is interesting to note that $\sigma_x^c/\sigma_x^* = 0.0177$ and $\sigma_y^c/\sigma_x^* = 0.0024$ for a steel beam; such low coating stresses (relative to calibration beam stresses) prevail only for $\theta \approx 0$ deg for the composite material. The coating stress transverse to the beam axis is compressive in the case of the graphite-epoxy composite up to about $\theta = 57$ deg.

The variation of the angle between the major reinforcement direction and the major principal strain direction with the angle between the major reinforcement direction and the calibration beam axis is shown in Fig. 2. The difference between the two angles is considerable for θ' between 0 and 60 deg.

The failure conditions given by Eqs. (10-12) depend on the fiber orientation angle θ. These equations are plotted in Figs. 3, 4, and 5 for $\theta = 0$, 45, and 90 deg, respectively, for $K = 4$. It should be noted that the scales are different in these figures. For $\theta = 0$ and 90 deg, the failure envelopes are similar to those for isotropic materials. For the 45 deg orientation, the failure envelope is very narrow and close to the line of symmetry, which is at 45 deg as for isotropic materials.

It is thus seen that the failure of the brittle coating is influenced by the biaxiality of the stress field in the composite structure that is being determined. An exact analysis is much more difficult in the case of the composite structure as the failure envelope is different for each angle of fiber orientation. However, the approximate analysis, based on Eq. (1), can still be performed on a composite structure and the accurate information regarding the principal strain directions can be used in conjunction with other experimental methods, such as strain gaging.

References

[1] Dally, J. W. and Prabhakaran, R., "Photo-Orthotropic-Elasticity, Parts I and II," *Experimental Mechanics*, Vol. 11, Aug. 1971, pp. 346-356.

[2] Dally, J. W. and Riley, W. F., *Experimental Stress Analysis*, McGraw-Hill Book Company, New York, 1965.

[3] Jones, R. M., *Mechanics of Composite Materials*, McGraw-Hill Book Company, New York, 1975.

Filtered Azimuthal Correlations in the Acoustic Far Field of a Subsonic Jet

Daniel Juvé,* Michel Sunyach,† and Geneviève Comte-Bellot‡
Ecole Centrale de Lyon, Ecully, France

Introduction

THE azimuthal structure of the acoustic field of circular jets has recently drawn the attention of several workers. For the near field, Armstrong et al.[1] have studied the coherence between two microphones placed on a circle centered on the jet axis; the spatial Fourier analysis of the coherence has shown that the major part of the energy is concentrated in the first three azimuthal modes. In the far field, azimuthal cross correlations have been measured by Maestrello[2] for a large range of Mach numbers ($0.6 \lesssim M \lesssim 1$), and by Juvé and Sunyach[3] for $M = 0.4$, but only *broad-band* results are available. Interpretations in terms of azimuthal modes have been attempted by Fuchs and Michel[4] for two values of the observation angle θ to the jet axis, $\theta = 30$ deg and $\theta = 60$ deg. A much more extensive analysis including $\theta = 90$ deg is given in Ref. 3. In the vicinity of the jet axis the first two modes ($m = 0,1$) give a satisfactory description of the acoustic field, but when the observation angle is increased more modes have to be taken into account, mode $m = 2$ being especially significant.

Since the last result may be misinterpreted because of the increase with θ of the high-frequency components in the acoustic spectra, we report in this Note some results concerning the *filtered* cross correlations between circumferentially displaced microphones in the acoustic far field and the associated modal expansion.

Test Facilities

Measurements have been conducted in the anechoic room of the Ecole Centrale de Lyon (ECL), with a cold jet of exit diameter 2 cm and velocity 135 m/s ($M = 0.4$). Two microphones (B & K 4133, Ø 1.27 cm) have been set on a circle centered on the $0x_1$ axis of the jet, the azimuthal spacing being denoted by φ (Fig. 1). The pressure signals are filtered by two band proportional analyzers (B & K 2107, $\Delta f/f = 0.29$) and fed to a digital correlator (HP 3721 A). The spatial cross-correlation coefficients $\tilde{R}_{p1p2}(\theta, \varphi, f)$ have been obtained for three typical values of the observation angle $\theta = 30$, 60, and 90 deg, the distance between the microphones and the nozzle being, respectively, 100, 80, and 60 diam. The results obtained for three frequencies corresponding to Strouhal numbers ($St = fD/U$) of 0.15, 0.3, and 0.6 are reported here, as these values are representative of those which contribute most to the noise spectrum.

Results

It has been checked, through space-time correlations, that the acoustic field is homogeneous in the azimuthal direction and nonswirling around $0x_1$. The correlation coefficient $\tilde{R}_{p1p2}$ is then a periodic and even function of the azimuthal spacing φ, which can be developed as an azimuthal Fourier series:

$$\tilde{R}_{p1p2}(\theta, \varphi, f) = \sum_{m=0}^{\infty} \tilde{a}_m(\theta, f) \cos m\varphi$$

with

$$\sum_{m=0}^{\infty} \tilde{a}_m(\theta, f) = 1$$

the $\tilde{a}_m$ coefficient represents the contribution of mode m to the acoustic energy for a given observation angle θ and frequency f. Such an expansion has been introduced by Michalke and Fuchs[5] as a basis for a theory on the noise generated by circular jets derived from Lighthill's acoustic analogy. This approach is of some interest only when a few modes are sufficient to correctly describe the pressure field, which is what we are looking for.

In Figs. 2-4 the results for the three observation angles are given. Our previous broad-band data[3] have been included for comparison.

For $\theta = 30$ deg, the $\tilde{R}_{p1p2}$ correlation decreases monotonically with φ, whatever the Strouhal number, the pressure fluctuations being almost "in phase" on the whole circumference of the jet. From the modal point of view, modes of order 0 (axisymmetric) and 1 (antisymmetric) are largely dominant. When the frequency is raised, a slight

Received Aug. 8, 1978.
Index categories: Aeroacoustics; Jets, Wakes, and Viscid-Inviscid Flow Interactions.

*Research Assistant, Mécanique des Fluides.
†Assistant Professor, Mécanique des Fluides.
‡Professor, Mécanique des Fluides.